ELSEVIER

Inorganica Chimica Acta 229 (1995) 307–313

Inorganica Chimica Acta

Cycloheptatrienyl bridged heterobimetallic complexes: fluxional behavior and X-ray crystal structure of *syn*-(μ^3:η^2-C_7H_7)Fe(CO)$_3$Pd(η^3-C_3H_5) ☆

Wenyi Fu [a], Robert McDonald [a], Josef Takats [a,*], Andrew H. Bond [b], Robin D. Rogers [b]

[a] *Department of Chemistry, University of Alberta, Edmonton, Alta., T6G 2G2, Canada*
[b] *Department of Chemistry, Northern Illinois University, DeKalb, IL 60115, USA*

Received 30 June 1994; revised 20 September 1994

Abstract

The structure and fluxionality of (μ-C_7H_7)Fe(CO)$_3$Pd(η^3-C_3H_5) are described. In solution the molecule is fluxional. Although ring whizzing of the C_7H_7 ring is still rapid, allyl group fluxionality is stopped at low temperature. ^{1}H and ^{13}C NMR spectra indicate an asymmetric ground state structure. This is confirmed by X-ray crystallography which shows that this is the second example of a μ-η^3:η^2 bonding for a bridging cycloheptatrienyl moiety, i.e. one double bond of the ring remains uncoordinated. Crystal data for *syn*-(μ-η^3:η^2-C_7H_7)Fe(CO)$_3$Pd(η^3-C_3H_5): monoclinic, space group $P2_1/n$, $a = 8.486(1)$, $b = 22.105(4)$, $c = 14.018(4)$ Å, $\beta = 104.84(2)°$, $V = 2542(2)$ Å^3, $Z = 8$, $R = 0.037$ and $R_w = 0.051$ based on 2482 reflections with $I \geqslant 3\sigma(I)$.

Keywords: Crystal structures; Iron complexes; Palladium complexes; Allyl complexes; Heterobimetallic complexes; Fluxional behavior; Bridging cycloheptatrienyl

1. Introduction

The chemistry of mononuclear cycloheptatriene (C_7H_8) and cycloheptatrienyl (C_7H_7) complexes is well established [1,2], and the number of cycloheptatrienyl bridged bimetallic complexes is steadily growing [3–6]. Although the mode of bonding of the μ-C_7H_7 moiety in the latter complexes is varied, a common feature is the attachment of all seven carbons to the bimetallic framework. Recently, Deganello and co-workers reported the unique structure of *syn*-(μ-η^3:η^2-C_7H_7)-Fe(CO)$_3$Pd(η^5-C_5H_5) in which a double bond of the bridging C_7H_7 ring remains uncoordinated [7]. In our systematic studies of cycloheptatrienyl bridged heterobimetallic complexes we were led to investigate the synthesis and properties of (μ-C_7H_7)MPd (M = Fe, Ru, Os) containing species [8]. Here we report on the fluxional behavior and structure of (μ-C_7H_7)Fe(CO)$_3$Pd(η^3-C_3H_5) (**1**), a compound previously prepared and assumed to contain a fully bonded μ-C_7H_7 moiety [5,7].

2. Experimental

All experimental procedures were performed in standard Schlenk glassware under a static atmosphere of rigorously purified nitrogen. All solvents were dried by refluxing under nitrogen with the appropriate drying agent and distilled just prior to use.

Potassium tertiarybutoxide (KO^{t}Bu) was purchased from Aldrich and sublimed prior to use (150 °C, 10^{-3} mm Hg). [(η^3-C_3H_5)PdCl]$_2$ [9] and (η^4-C_7H_8)Fe(CO)$_3$ [10] were prepared according to literature methods.

IR spectra were obtained with a Bomem MB-100 FTIR spectrometer (hexane solution in 0.1 mm path length KBr solution cell). Mass spectra were taken with an A.E.I. MS-12 spectrometer operating at 70 eV. NMR spectra were recorded on a Bruker WH 200, Bruker WH 360 or Bruker AM 300 spectrometer using flame sealed NMR tubes. Elemental analyses were performed by the Microanalytical Laboratory of this department.

☆ This article is dedicated to Professor F.A. Cotton on the occasion of his 65th birthday. Many thanks for opening the authors' eyes to the fascinating world of fluxional organometallic molecules.

* Corresponding author.

SSDI 0020-1693(94)04259-X

2.1. Preparation of $[(\mu\text{-}C_7H_7)Fe(CO)_3Pd(\eta^3\text{-}C_3H_5)]$ (1)

$K[(\eta^3\text{-}C_7H_7)Fe(CO)_3]$ was prepared from $(\eta^4\text{-}C_7H_8)Fe(CO)_3$ (1.29 g, 5.57 mmol; 20 ml THF) and KO^{t}Bu (625 mg, 5.57 mmol; 12 ml THF) at room temperature. The reaction was monitored by IR spectroscopy. The red anion solution was cooled to −78 °C and was added dropwise to a stirred solution of $[(\eta^3\text{-}C_3H_5)PdCl]_2$ (1.0 g, 2.78 mmol) in 40 ml of THF kept at 0 °C. After the addition was complete, the mixture was allowed to slowly warm to room temperature overnight. The IR spectrum showed complete consumption of the anion. Solvent was removed under vacuum affording a dark red oil. The residue was extracted with hexane (30 ml and 5×5 ml). The combined extracts were concentrated to ~10 ml and cooled to −20 °C to give dark red crystalline $(\mu\text{-}C_7H_7)Fe(CO)_3Pd(\eta^3\text{-}C_3H_5)$ (**1**) (630 mg, 33%). *Anal.* Calc. for $C_{13}H_{12}O_3FePd$: C, 41.25, H, 3.20. Found: C, 41.07, H, 3.20%. Mass spectrum (70 eV, 110 °C): M^+ (378), $M^+ - n$CO (n = 1–3). IR (hexane): ν(CO) 2003vs, 1945s, 1934s cm^{-1}. ^{1}H NMR (22 °C, $CDCl_3$): δ 4.76 (s, 7H, C_7H_7), 5.34 (tt, J_{23} = 7 Hz, J_{13} = 13 Hz, H_3-allyl), 4.70 (d, J_{23} = 7 Hz, 2H, $H_{2,4}$-allyl), 3.14 (d, J_{13} = 13 Hz, 2H, $H_{1,5}$-allyl); (−60 °C, $CDCl_3$): δ 4.78 (s, 7H, C_7H_7), 5.34 (tt, J_{23} = 7 Hz, J_{13} = 13 Hz, H_3), 5.00 (d, J = 7 Hz, 1H, $H_{2\text{ or }4}$), 4.40 (d, J = 7 Hz, 1H, $H_{2\text{ or }4}$), 3.20 (d, J = 13 Hz, 1H, $H_{1\text{ or }5}$), 2.90 (d, J = 14 Hz, 1H, $H_{1\text{ or }5}$). $^{13}C\{^1H\}$ NMR (25 °C, CD_2Cl_2): δ 84.86 (s, C_7H_7), 113.74 (s, allyl *C*H), 70.51 (s, allyl CH_2) 220.20 (s, CO_{Fe}); (−50 °C, $CDCl_3$): δ 84.19 (s, C_7H_7), 113.74 (s, allyl *C*H), 70.10 (s, allyl CH_2), 71.07 (s, allyl CH_2), 220.20 (s, CO_{Fe}).

2.2. Crystal structure determination of $[(\mu\text{-}C_7H_7)Fe(CO)_3Pd(\eta^3\text{-}C_3H_5)]$ (1)

Deep red–purple crystals of complex **1** were grown from hexane solution at −20 °C. One of these, with the approximate dimensions of 0.76×0.39×0.10 mm, was mounted in a glass capillary for use in X-ray data collection. The automatic peak search and reflection indexing programs [1] generated a monoclinic cell. The systematic absences ($h0l$, $h+l$ odd; $0k0$, k odd) led to the choice of space group as $P2_1/n$, a non-standard setting of $P2_1/c$ (No. 14) [11]. The cell constants and orientation matrix were obtained from a least-squares refinement of the setting angles of 24 reflections in the range $18.2 \leqslant 2\theta \leqslant 26.0°$. The unit cell parameters are given in Table 1.

In Table 1 the conditions used for intensity data collection are summarized. The backgrounds for the peaks were measured by extending the scan by 25% on either side of the calculated range, giving a peak-to-background counting time ratio of 2:1. Three reflections were chosen as intensity and orientation standards, and these were remeasured after every 120 min of exposure time to check on crystal and electronic stability over the course of data collection; no appreciable decay was evident.

The positions of most of the non-hydrogen atoms of the molecule were found using the direct-methods program SHELXS-86 [12]. The remaining non-hydrogen atoms were located from a series of difference Fourier maps. Adjustment [13] of atomic parameters was carried out by full-matrix least-squares refinement on F_o minimizing the function $\Sigma w(|F_o| - |F_c|)^2$, where the weighting factor w is $4F_o^2/\sigma^2(F_o^2)$. The neutral atom scattering

Table 1
Crystallographic data for *syn*-$(\mu\text{-}\eta^3\text{:}\eta^2\text{-}C_7H_7)Fe(CO)_3Pd(\eta^3\text{-}C_3H_5)$ (**1**)

Crystal data	
Formula	$C_{13}H_{12}FeO_3Pd$
Formula weight	378.49
Crystal dimensions (mm)	0.76×0.39×0.10
Space group	$P2_1/n$ (a non-standard setting of $P2_1/c$ (No. 14))
Unit cell parameters	
a (Å)	8.486(1)
b (Å)	22.105(4)
c (Å)	14.018(4)
β (°)	2542(2)
V (Å^3)	104.84(2)
Z	8
ρ_{calc} (g cm^{-3})	1.978
μ (cm^{-1})	25.34
Data collection and refinement conditions	
Diffractometer	Enraf-Nonius CAD4
Temperature (°C)	−50
Radiation (λ (Å))	Mo Kα (0.71073)
Monochromator	incident beam, graphite crystal
Take-off angle (°)	3.0
Detector aperture (mm)	(3.00+tan θ) horiz ×4.00 vert
Crystal-to-detector distance (mm)	173
Scan type	θ–2θ
Scan rate (° min^{-1})	6.7–1.2
Scan width (°)	0.60+0.347 tan θ
Data collection 2θ limit (°)	50.0
Total data collected	4098 ($+k \pm k \pm l$)
Range of absorption correction factors	0.8614–1.2267
Total unique data	3940
No. observations (NO)	2482 ($I > 3.0\sigma(I)$)
Final no. parameters varied (NV)	325
R [a]	0.037
R_w [b]	0.051
GOF [c]	1.554

[a] $R = \Sigma||F_o| - |F_c||/\Sigma|F_o|$.
[b] $R_w = [\Sigma w(|F_o| - |F_c|)^2/(\Sigma w F_o^2)]^{1/2}$.
[c] $GOF = [\Sigma w(|F_o| - |F_c|)^2/(NO - NV)]^{1/2}$.

[1] The diffractometer programs are those supplied by Enraf-Nonius for operating the CAD4 diffractometer.

factors [14a] and anomalous dispersion terms [14b] were taken from the usual tabulations. Hydrogen atoms were not refined, but were generated at idealized calculated positions by assuming a C–H bond length of 0.95 Å and the appropriate sp^2 or sp^3 geometry, and were given fixed, isotropic Gaussian displacement parameters 1.2 times those of the attached atoms. After refinement of the coordinates and isotropic U values for all non-hydrogen atoms had converged, the data were corrected for absorption by use of the method of Walker and Stuart (DIFABS) [15]. All non-hydrogen atoms were given anisotropic thermal parameters. For a summary of the final agreement indices see Table 1.

The final atomic coordinates and equivalent isotropic displacement parameters are listed in Table 2.

Table 2
Atomic coordinates and equivalent isotropic displacement parameters of non-hydrogen atoms for *syn*-(μ-η^3:η^2-C_7H_7)Fe(CO)$_3$Pd(η^3-C_3H_5) (**1**) [a,b]

Atom [c]	x	y	z	B_{eq} (Å^2)
PdA	0.30373(9)	0.19207(4)	0.27101(5)	2.28(2)*
FeA	0.1687(2)	0.21790(7)	0.41887(9)	2.31(3)*
O14A	0.2729(8)	0.0927(3)	0.4292(5)	3.5(2)*
O15A	−0.0087(9)	0.2005(4)	0.5700(5)	4.6(2)*
O16A	−0.1333(8)	0.2197(3)	0.2597(5)	3.6(2)*
C11A	0.161(1)	0.1196(5)	0.1893(7)	3.7(3)*
C12A	0.319(1)	0.1166(5)	0.1809(7)	3.2(3)*
C13A	0.385(1)	0.1645(5)	0.1420(7)	3.8(3)*
C14A	0.235(1)	0.1425(4)	0.4188(6)	2.3(2)*
C15A	0.063(1)	0.2098(5)	0.5102(7)	2.9(3)*
C16A	−0.014(1)	0.2191(5)	0.3210(7)	2.9(3)*
C21A	0.494(1)	0.2628(5)	0.3243(8)	3.5(3)*
C22A	0.340(1)	0.2898(5)	0.3104(8)	3.4(3)*
C23A	0.248(1)	0.3053(5)	0.3118(8)	3.7(3)*
C24A	0.289(1)	0.2928(5)	0.4827(9)	4.5(3)*
C25A	0.390(1)	0.2435(5)	0.5247(7)	3.5(3)*
C26A	0.544(1)	0.2279(5)	0.4962(8)	3.4(3)*
C27A	0.591(1)	0.2377(5)	0.4153(8)	3.2(3)*
PdB	0.30292(8)	0.00443(3)	0.67583(5)	2.07(2)*
FeB	0.1991(1)	0.05157(6)	0.82336(9)	2.09(3)*
O14B	0.2622(9)	−0.0782(3)	0.8626(5)	3.8(2)*
O15B	0.0131(8)	0.0713(4)	0.9699(5)	5.1(2)*
O16B	−0.0985(8)	0.0604(4)	0.6642(5)	5.0(2)*
C11B	0.128(1)	−0.0648(5)	0.6198(7)	3.4(3)*
C12B	0.281(1)	−0.0815(5)	0.6061(7)	3.2(3)*
C13B	0.354(1)	−0.0439(5)	0.5501(7)	3.3(3)*
C14B	0.237(1)	−0.0277(5)	0.8433(6)	2.5(3)*
C15B	0.091(1)	0.0649(5)	0.9150(7)	3.0(3)*
C16B	0.022(1)	0.0561(5)	0.7259(6)	2.8(2)*
C21B	0.514(1)	0.0681(4)	0.7073(6)	2.2(2)*
C22B	0.370(1)	0.1017(4)	0.6949(6)	2.6(2)*
C23B	0.298(1)	0.1294(4)	0.7661(7)	2.4(2)*
C24B	0.349(1)	0.1223(4)	0.8701(7)	2.4(2)*
C25B	0.439(1)	0.0726(4)	0.9144(6)	2.1(2)*
C26B	0.576(1)	0.0461(4)	0.8865(7)	2.7(3)*
C27B	0.614(1)	0.0450(4)	0.7978(7)	2.4(3)*

[a] Numbers in parentheses are e.s.d.s in the least significant digit.
[b] Anisotropically-refined atoms are marked with an asterisk (*). Displacement parameters for the anisotropically refined atoms are given in the form of the equivalent isotropic Gaussian displacement parameter B_{eq}, defined as $4/3[a^2\beta_{11}+b^2\beta_{22}+c^2\beta_{33}+ab\ (\cos\gamma)\beta_{12}+ac\ (\cos\beta)\beta_{13}+bc\ (\cos\alpha)\beta_{23}]$.
[c] In this Table and elsewhere, the corresponding atoms of the two independent molecules are given the same numerical numbers; the two molecules are distinguished by the letter designation A and B.

3. Results and discussion

Reaction of K[(η^3-C_7H_7)Fe(CO)$_3$] with [(η^3-C_3H_5)PdCl]$_2$ proceeds as described previously for the Li^+ salt by Salzer et al. [5] and gives (μ-C_7H_7)Fe(CO)$_3$Pd(η^3-C_3H_5) (**1**) in similar (33%) yield. In this connection it is worthy of note that by using the cationic palladium source, [(η^4-1,5-C_8H_{12})Pd(η^3-C_3H_5)]BF_4, Deganello and co-workers have increased the isolated yield of **1** to 50% [7]. Compound **1** is moderately air stable and soluble in most organic solvents. However in solution at room temperature, even under an inert atmosphere, it decomposes to a black solid.

3.1. Fluxional behavior of 1

The spectroscopic data for **1** are in good agreement with the previous reports [5,7]. The IR spectrum shows three terminal CO stretching bands at 2003vs, 1945s, 1934s cm^{-1}. At ambient temperature both ^1H and ^{13}C NMR spectra show a single, time-averaged signal for the C_7H_7 ring at 4.76 and 84.86 ppm, respectively. Interestingly, the chemical shifts are very similar to those reported by Deganello and co-workers [7] (4.72 and 82.2 ppm) for the cycloheptatrienyl bridged Fe–Pd complex, *syn*-(μ-η^3:η^2-C_7H_7)Fe(CO)$_3$Pd(η^5-C_5H_5) (**2**), in which a double bond of the μ-C_7H_7 ligand remains uncoordinated.

The simple, three-signal pattern for the η_3-allyl group with a 2:2:1 ratio (Fig. 1) indicates that the allyl group is fluxional as well. Based on signal intensity, the multiplet at 5.34 ppm (J=7 and 13 Hz) is assigned to the central proton, H_3 which shows coupling to the other two types of protons. The remaining two doublets are assigned to the *syn* protons, H_2/H_4 (4.67 ppm, J=7 Hz) and *anti* protons, H_1/H_5 (3.07 ppm, J=13 Hz) on the basis of coupling considerations (smaller coupling for the two *syn* protons and larger coupling for two *anti* protons).

To investigate the fluxional behavior of **1** a variable temperature NMR study was carried out. The single C_7H_7 resonance remains sharp even at −80 °C, and indicates rapid ring whizzing in this molecule. The high fluxionality of the C_7H_7 ring is consistent with the expected *syn*-(μ-C_7H_7)Fe(CO)$_3$Pd(η^3-C_3H_5) formulation, since rapid ring whizzing is typical for *syn*-cycloheptatrienyl bridged bimetallic complexes [4,5], except for a few compounds such as *syn*-(μ-C_7H_7)Ru-

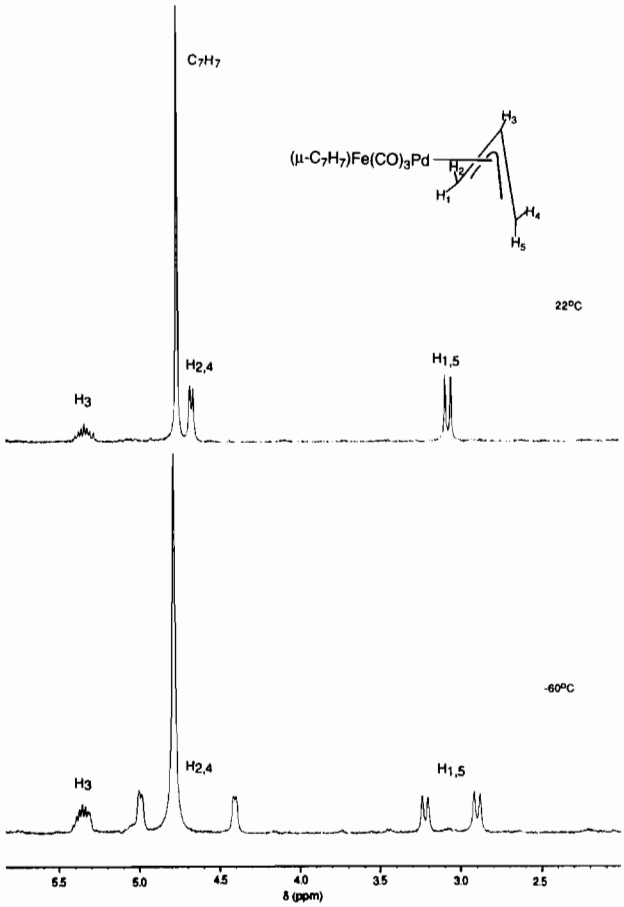

Fig. 1. Variable temperature ^1H NMR spectra (360 MHz) of (μ-C_7H_7)$Fe(CO)_3Pd(\eta^3$-C_3H_5) (**1**) in $CDCl_3$.

$(CO)_3Ir(CO)_2$ [4f], *syn*-(μ-C_7H_7)$Os(CO)_3M(\eta^4$-C_8H_{12}) (M = Rh, Ir) [16] and *syn*-(μ-η^3:η^2-C_7H_7)$Fe(CO)_3Pd(\eta^5$-C_5H_5) (**2**) whose ring whizzing can be frozen out at low temperature. It is noteworthy that the fluxionality of **1** is much higher than that of complex **2**. Indeed in that case the low temperature limiting ^1H and ^{13}C NMR spectra are reached at −90 and −80 °C, respectively. In accord with the higher rate of ring whizzing carbonyl scrambling is also faster in **1**. The single time averaged CO signals, due to the $Fe(CO)_3$ moiety, persist down to low temperature whereas in complex **2** a three-line pattern is seen already at −40 °C.

Contrary to the very rapid ring whizzing of the C_7H_7 moiety the NMR signals of the allyl group undergo changes as the temperature is lowered. The signals broaden and decoalesce at −30 °C. The low temperature limiting ^1H NMR spectrum for the allyl group is obtained at −60 °C and shows five signals, each corresponding to one proton. The central proton H_3 remains at 5.34 ppm without significant changes, but the signals due to the four terminal protons split into four signals. Based on the coupling constants, the two downfield peaks (5.00 and 4.40 ppm) are assigned to the *syn* protons H_2/H_4 and the two upfield signals (3.20 and 2.90 ppm) to the *anti* protons H_1/H_5. Assignments of these signals to specific hydrogen atoms from NOE experiments at −70 °C were not successful. However, the observation of five proton signals suggests that the ground state structure of **1** is such that it allows for an asymmetric orientation of the allyl group.

The fluxional allyl group and its asymmetric orientation were confirmed by the variable temperature ^{13}C NMR spectroscopy. At ambient temperature, only two peaks are observed for the allyl ligand, one for the central carbon atom at 113.74 ppm and another for the terminal carbon atoms at 70.51 ppm. At −50 °C the latter signal splits into two equal intensity peaks at 70.10 and 71.07 ppm, respectively, giving further evidence for the non-equivalence of the two terminal carbon atoms of the allyl ligand at low temperature.

3.2. Molecular structure of 1

In the absence of a low temperature limiting spectrum for the C_7H_7 moiety and in view of the unexpected asymmetric disposition of the allyl ligand on the Pd center it was deemed necessary to carry out a single-crystal X-ray analysis of complex **1** in order to ascertain the bonding mode of the μ-C_7H_7 ring and to deduce the precise geometry of the molecule. Two perspective views of **1** with the numbering scheme are shown in Fig. 2. The compound crystallizes with two crystallographically-independent molecules per asymmetric unit; only one of the independent molecules is shown in Fig. 2. For ease of readability and comparison the equivalent atoms are given the same numerical numbers and are distinguished by the letter designation A and B. The metrical parameters of the two molecules are similar. In our discussion we normally use the average of the corresponding values; individual distances and angles will be mentioned only when they are significantly different. Selected bond distances and angles are listed in Table 3.

It is clear from Fig. 2 that the X-ray analysis confirms the anticipated *syn*-(μ-C_7H_7)FePd core, however, contrary to previous assumptions [5,7] the Pd center is bonded to only *one* double bond (C21–C22) of the C_7H_7 ring, leaving another double bond (C26–C27) free. Complex **1** thus represents the second example of a molecule featuring the (μ-η^3:η^2-C_7H_7) moiety, the other being Deganello's *syn*-(μ-η^3:η^2-C_7H_7)$Fe(CO)_3Pd(\eta^5$-C_5H_5) (**2**). The major difference between the two complexes is that in **2** both Fe and Pd atoms achieve the favored 18-electron configuration, whereas in **1** Pd has only 16 valence electrons. For electron counting purposes we may adopt the charge distribution proposed by Salzer et al. [5] in these heterobimetallic complexes, with the negative charge concentrated on the (allylic)$Fe(CO)_3$ fragment and the positive charge on the

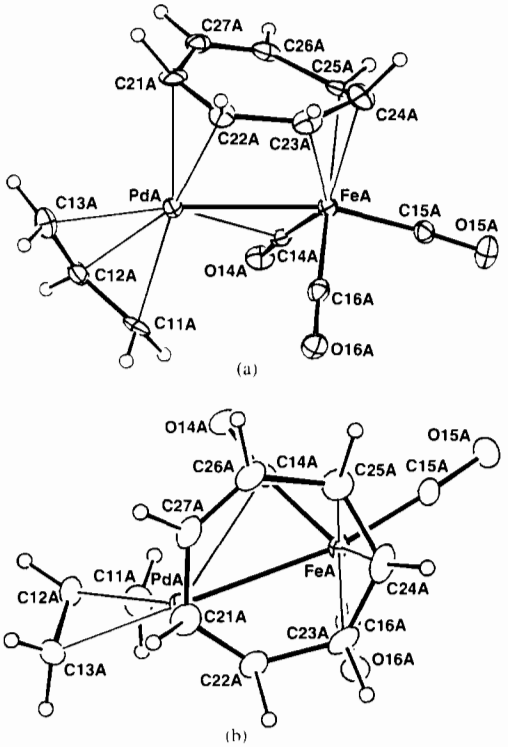

Fig. 2. (a) Perspective view of one of the two crystallographically-independent *syn*-(μ-η^3:η^2-C_7H_7)Fe(CO)$_3$Pd(η^3-C_3H_5) molecules in the unit cell, showing the atom labeling scheme. Non-hydrogen atoms are represented by Gaussian ellipsoids at the 20% probability level; hydrogens are shown artificially small. (b) Alternate view of the molecule from above the C_7H_7 ring.

(allyl)Pd(olefin) part. Palladium is thus in its common Pd(II)(d^8) oxidation state and achieves a 16-electron configuration by formation of a Fe → Pd donor–acceptor bond. Of course the alternative consideration of a normal Fe–Pd single bond [7] would also result in 18(Fe) and 16(Pd) valence electron counts. The coordination geometries around Fe can be described as 'six-coordinate'; with three carbonyl groups, and the allylic fragment (C23–C24–C25) and the Fe–Pd bond forming opposite triangular faces of a distorted octahedron. Whereas Pd is 'four-coordinate' with the mid-point of the double bond (C21–C22), the Pd–Fe bond and the allyl ligand (C11–C12–C13) defining a 'square' planar arrangement. The observed asymmetric structure is in agreement with the low temperature NMR spectra which show five distinct allyl-H resonances and three allyl-C signals.

In view of the similarity between **1** and **2** it is instructive to compare the corresponding metrical parameters. The Fe–Pd bond lengths (2.674(1) and 2.659(11) Å) are close to that observed for **2** (2.653(1) Å). The distances of Fe to the allylic part of the C_7H_7 ring are in the range 2.153(9)–2.015(8) Å which is also close to those found in **2**, 2.18–2.06 Å, and the commonly observed pattern of long–short–long Fe–C(ring) interaction is also maintained. However, the strength of the Pd–double bond interaction (Pd–C21AC22A/C21BC22B) in **1** appears to be weaker than in **2** as the bond distances are longer (av. Pd–C distance 2.230(4) Å in **1** versus 2.151(3) Å in **2**). On the other hand the Pd–allyl distances are typical [17].

Table 3
Selected bond lengths (Å) and angles (°) for **1**

Bond lengths			
PdA–FeA	2.674(1)	PdB–FeB	2.659(1)
PdA–C11A	2.154(8)	PdB–C11B	2.136(8)
PdA–C12A	2.117(8)	PdB–C12B	2.123(8)
PaA–C13A	2.182(9)	PdB–C13B	2.195(8)
PdA–C14A	2.538(8)	PdB–C14B	2.645(8)
PdA–C21A	2.235(8)	PdB–C21B	2.231(7)
PdA–C22A	2.232(9)	PdB–C22B	2.224(8)
FeA–C14A	1.76(1)	FeB–C14B	1.79(1)
FeA–C15A	1.752(8)	FeB–C15B	1.785(9)
FeA–C16A	1.785(9)	FeB–C16B	1.754(8)
FeA–C23A	2.153(9)	FeB–C23B	2.158(8)
FeA–C24A	2.027(9)	FeB–C24B	2.015(8)
FeA–C26A	2.149(8)	FeB–C25B	2.157(7)
O14A–C14A	1.146(9)	O14B–C14B	1.15(1)
O15A–C15A	1.172(9)	O15B–C15B	1.144(9)
O16A–C16A	1.151(9)	O16B–C16B	1.164(9)
C11A–C12A	1.38(1)	C11B–C12B	1.41(1)
C12A–C13A	1.37(1)	C12B–C13B	1.39(1)
C21A–C22A	1.41(1)	C21B–C22B	1.40(1)
C21A–C27A	1.44(1)	C21B–C27B	1.43(1)
C22A–C23A	1.46(1)	C22B–C23B	1.43(1)
C23A–C24A	1.40(1)	C23B–C24B	1.42(1)
C24A–C25A	1.42(1)	C24B–C25B	1.39(1)
C25A–C26A	1.50(1)	C25B–C26B	1.44(1)
C26A–C27A	1.31(1)	C26B–C27B	1.36(1)
Bond angles			
FeA–C14A–O14A	171.6(7)	FeB–C14B–O14B	175.5(7)
FeA–C15A–O15A	175.7(8)	FeB–C15B–O16B	175.4(8)
FeA–C16A–O16A	178.3(7)	FeB–C16B–O16B	176.8(7)
PdA–FeA–C14A	66.2(2)	PdB–FeB–C14B	69.8(3)
PdA–FeA–C16A	82.3(3)	PdB–FeB–C16B	78.7(3)
C11A–C12A–C13A	120.1(9)	C11B–C12B–C13B	118.4(9)
C21A–C22A–C23A	130.3(9)	C21B–C22B–C23B	130.8(7)
C22A–C23A–C24A	127.8(8)	C22B–C23B–C24B	126.7(7)
C23A–C24A–C25A	122.6(8)	C23B–C24B–C25B	122.2(7)
C24A–C25A–C26A	122.8(9)	C24B–C25B–C26B	126.1(7)
C25A–C26A–C27A	131.9(8)	C25B–C26B–C27B	130.6(7)
C26A–C27A–C21A	126.9(8)	C26B–C27B–C21B	125.2(7)
C27A–C21A–C22A	125.8(8)	C27B–C21B–C22B	127.0(7)

As mentioned, the major difference between the two complexes is the electronic nature of the Pd centers, saturated in **2** while remaining unsaturated in **1**. The unsaturated nature of Pd in complex **1** appears not to be relieved by additional interaction with the uncoordinated double bond of the ring (C27–C26); these distances are long (Pd–C27 2.92 Å; Pd–C26 3.38 Å). However the presence of a semi-bridging carbonyl group may fulfill this purpose. Deganello and co-workers [7] noted that one of the carbonyl ligands in complex **2** has a 'slightly semi-bridging character' (Fe–C–O angle of 171.0(3)° and Pd···C separation of 2.653(4) Å). In view of the unsaturated nature of Pd in **1** it may be anticipated that the semi-bridging interaction will be

stronger. This is indeed the case for one of the independent molecules (PdA–C14A 2.538(8) Å; FeA–C14A–O14A 171.6(7)°). However, and unexpectedly, the semi-bridging interaction in the other molecule is significantly different. The PdB–C14B distance of 2.645(8) Å is 13σ longer than the PdA–C14A distance and resembles that observed in complex **2**. It is interesting to note that the difference in semi-bridging character manifests itself in a shorter PdB–FeB contact of 2.659(1) Å versus the significantly longer PdA–FeA separation of 2.674(1) Å. Thus the decrease in semi-bridging carbonyl character is accompanied by a decrease in the Pd–Fe distance; in either case the Pd center is seeking to stabilize its electron deficiency. Of course the compensating effects are not the reason for the differences observed in this part of the two independent molecules and we have no rational explanation to offer for the phenomenon and even solid state effects cannot be ruled out since the solution IR spectrum of the complex reveals only terminal CO bands. Of course, it is an accepted paradigm of organometallic chemistry that semi-bridging carbonyls represent a continuum between terminal and fully bridged CO groups [18]; slight energetic changes may produce significant movement of the carbonyl moiety.

As a result of the μ-η^3:η^2 bonding the C_7H_7 ring can be divided into three parts, 'allylic' (av. C–C 1.41(1) Å), and coordinated and free double bonds (av. C–C 1.40(1) and 1.34(2) Å, respectively) which are separated by longer C–C bonds (av. C–C 1.46(1) Å). The corresponding distances in complex **2** are similar (1.404, 1.406, 1.331 and 1.444 Å, respectively). The C_7H_7 ring is not planar, the average torsional angles between the free double bond and the allylic moiety, the coordinated double bond and the allylic moiety, and the free and coordinated double bonds are 27, 7 and 9°, respectively (the corresponding values in complex **2** are 35, 24 and 13°). Thus it appears that the C_7H_7 ring is less distorted in **1** than in compound **2** and consequently the π electrons of the C_7H_7 ligand are slightly more delocalized in the former. This, coupled with the weaker bonding interaction between Pd and the coordinated double bond and the coordinatively unsaturated nature of the metal center in *syn*-(μ-η^3:η^2-C_7H_7)$Fe(CO)_3Pd(\eta^3$-C_3H_5) account for the enhanced fluxionality of the μ-C_7H_7 ligand in this complex compared to compound **2**.

4. Conclusions

The observed asymmetric ground state structure of (μ-C_7H_7)$Fe(CO)_3Pd(\eta^3$-C_3H_5) (**1**) was mildly surprising. On the basis of the 18-electron rule and the room temperature NMR spectra a symmetrical (μ-η^3:η^4-C_7H_7)FePd bonding was anticipated. However, the identification of the (μ-η^3:η^2-C_7H_7)FePd core with a 16-electron Pd center is not exceptional since the 16-electron configuration is widely observed in organo–palladium complexes [19].

Complex **1** features three distinct fluxional processes: C_7H_7 ring whizzing, allyl group rearrangements and carbonyl scrambling. Although it is probable that the unsaturated nature of Pd plays a role in the enhanced fluxionality of **1** compared to its saturated relative, *syn*-(μ-η^3:η^2-C_7H_7)$Fe(CO)_3Pd(\eta^5$-C_5H_5) (**2**), via an (η^2-C_7H_7)Pd/(η^4-C_7H_7)Pd interconversion (Scheme 1), it is clear from the observed line shape changes that metal migration is much more facile and independent of allyl group fluxionality. Indeed, as shown in the top row of Scheme 1, C_7H_7 ring whizzing which proceeds via rapid 1,2-metal shifts, through the intermediacy of an (η^4-C_7H_7)Pd intermediate or without such intervention, does not involve allyl group equilibration. This is in accord with the low temperature ^1H and ^{13}C NMR spectra which show averaged μ-C_7H_7 signals but distinct allyl group resonances. The higher energy *syn–syn* (H_2 and H_4) and *anti–anti* (H_1 and H_5) exchange can be accomplished by the well-known allyl rotation about the Pd–allyl bond axis [20]. As shown in the bottom row of Scheme 1, allyl rotation in the putative (η^4-C_7H_7)Pd intermediate would immediately exchange the *syn–syn* and *anti–anti* hydrogens. Alternatively a twitching motion between two enantiomorphous (η^2-C_7H_7)Pd structures, accompanied by allyl rotation would also accomplish the equilibration process. From the coalescence behavior of the ^1H NMR signals an activation barrier of 47 kJ mol^{-1} can be estimated [21] for the exchange process.

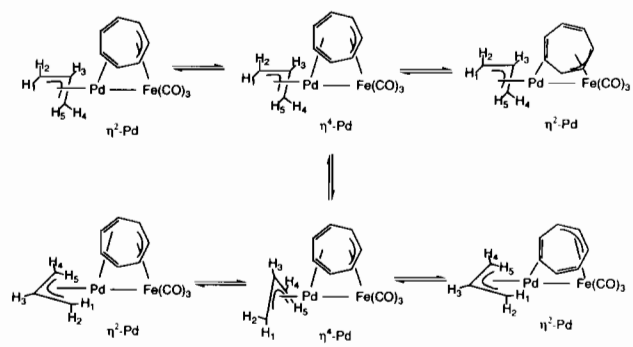

Scheme 1.

5. Supplementary material

Tables of anisotropic displacement parameters, derived atomic coordinates and isotropic displacement parameters for hydrogen atoms, bond and torsion angles involving non-hydrogen atoms, and observed and calculated structure factor amplitudes have been deposited at the Cambridge Crystallographic Data Center.

Acknowledgements

We thank the Natural Sciences and Engineering Research Council (Canada) and the University of Alberta for financial support. We also thank Professor M. Cowie of this department for use of his diffractometer for data collection.

References

[1] G. Deganello, *Transition Metal Complexes of Cyclic Polyolefins,* Academic Press, London 1979, Ch. 1.

[2] (a) L.K.K. LiShingMan and J. Takats, *J. Organomet. Chem., 117* (1976) C104; (b) J.G.A. Reuvers and J. Takats, *J. Organomet. Chem., 175* (1979) C13; (c) L.K.K. LiShingMan, J.G.A. Reuvers, J. Takats and G. Deganello, *Organometallics, 2* (1982) 28; (d) G.-Y. Kiel and J. Takats, *Organometallics, 6* (1987) 2009; (e) F. Edelmann, G.-Y. Kiel, J. Takats, A. Vasudevamurthy and M.-Y. Yeung, *J. Chem. Soc., Chem. Commun.,* (1988) 296; (f) S.T. Astley, J. Takats, J.C. Huffman and W.E. Streib, *Organometallics, 9* (1990) 184; (g) J.G.A. Reuvers and J. Takats, *Organometallics, 9* (1990) 578.

[3] F.A. Cotton and C.R. Reich, *J. Am. Chem. Soc., 91* (1969) 847.

[4] (a) M.J. Bennett, J.L. Pratt, K.A. Simpson, L.K.K. LiShingMan and J. Takats, *J. Am. Chem. Soc., 98* (1976) 810; (b) G.-Y. Lin and J. Takats, *J. Organomet. Chem., 269* (1984) C4; (c) R.G. Ball, R. Drews, F. Edelmann, G.-Y. Kiel and J. Takats, *Organometallics, 5* (1986) 829; (d) A. Vasudevamurthy and J. Takats, *Organometallics, 6* (1987) 2005; (e) F. Edelmann and J. Takats, *J. Organomet. Chem., 344* (1988) 351; (f) S.T. Astley and J. Takats, *J. Organomet. Chem., 363* (1989) 167.

[5] A. Salzer, T. Egolf and W. von Philipsborn, *Helv. Chim. Acta 65* (1982) 1145.

[6] H.J. Müller, U. Nagel, M. Steinmann, K. Polborn and W. Beck, *Chem. Ber., 122* (1989) 1387.

[7] M. Airoldi, G. Deganello, G. Gennaro, M. Moret and A. Sironi, *Organometallics, 12* (1993) 3964.

[8] W. Fu, *Ph.D. Thesis,* University of Alberta, Edmonton, Alta., Canada, 1993, Ch. 3.

[9] Y. Tatsuno, T. Yoshida and S. Otsuka, *Inorg. Synth., 19* (1979) 220.

[10] (a) R. Burton, L. Pratt and G. Wilkinson, *J. Chem. Soc.,* (1979) 594; (b) L. Kruczynski and J. Takats, *Inorg. Chem., 15* (1976) 3140.

[11] *International Tables for X-Ray Crystallography,* Vol. I, Kynoch, Birmingham, UK, 1969.

[12] G.M. Sheldrick, *Acta Crystallogr., Sect. A, 46* (1990) 467.

[13] *Structure Determination Package,* Version 3, Enraf-Nonius, Delft, Netherlands, 1985; adapted for a SUN SPARCstation 1+computer; and several locally written programs by R.G. Ball.

[14] *International Tables for X-Ray Crystallography,* Vol. IV, Kynoch, Birmingham, UK, 1974 (present distributor Reidel, Dordrecht, Netherlands); (a) Table 2.2B, (b) Table 2.31.

[15] N. Walker and D. Stuart, *Acta Crystallogr., Sect. A, 39* (1983) 158.

[16] S.T. Astley, *Ph.D. Thesis,* University of Alberta, Edmonton, Alta., Canada, 1989, Ch. 4.

[17] (a) A.E. Smith, *Acta Crystallogr., 18* (1965) 331; (b) M. Gassi, S.V. Meille, A. Musco, R. Pontellini and A. Sironi, *J. Chem. Soc., Dalton Trans.,* (1989) 615.

[18] (a) F.A. Cotton, *Prog. Inorg. Chem., 21* (1976) 1; (b) R. Colton and M.J. McCormick, *Coord. Chem. Rev., 31* (1980) 1; (c) C.P. Horwitz and D.F. Shriver, *Adv. Organomet. Chem., 23* (1984) 219; (d) R.H. Crabtree and M. Lavin, *Inorg. Chem., 25* (1986) 805.

[19] F.A. Cotton and G. Wilkinson, *Advanced Inorganic Chemistry,* Wiley, New York, 5th edn., 1988, Ch. 21 and 19-H.

[20] (a) K. Vrieze, in L.M. Jackman and F.A. Cotton (eds.), *Dynamic Nuclear Magnetic Resonance Spectroscopy,* Academic Press, New York, 1975, p. 441; (b) J.W. Faller, *Adv. Organomet. Chem., 16* (1977) 211.

[21] J. Sandstrom, *Dynamic NMR Spectroscopy,* Academic Press, London, 1982, p. 96.